Terra Nova
THE EUROPEAN JOURNAL OF GEOSCIENCES

Long-lasting intracontinental strike-slip faulting; new evidence from the Karakorum shear zone in the Himalayas.

Journal:	*Terra Nova*
Manuscript ID:	TER-2010-0108.R1
Wiley - Manuscript type:	Paper
Date Submitted by the Author:	n/a
Complete List of Authors:	Leloup, Philippe; CNRS, Laboratoire des sciences de la terre boutonnet, emmanuelle; Université Lyon 1, laboratoire des sciences de la terre Davis, bill; Geological Survey of Canada, ESS/GSC-CNCB/GSC-CC/GEOCHRON Hattori, Keiko; University of Ottawa
Keywords:	Strike-slip fault, Magmatism, Geochronology, Deformation, Karakorum

Long-lasting intracontinental strike-slip faulting; new evidence from the Karakorum shear zone in the Himalayas.

Running head: **Long lasting activity of the Karakorum fault.**

P.H. Leloup[1], E. Boutonnet[1], W.J. Davis[2], K. Hattori[3].

1 L.S.T. UMR CNRS 5570, Université Lyon 1, France.
tel: [33] (0)4 72 44 62 38 ; fax: [33] (0)4 72 44 85 93 ; Email: herve.leloup@univ-lyon1.fr
2 ESS/GSC-CNCB/GSC-CC/GEOCHRON, Geological Survey of Canada.
3 Department of Earth Sciences, University of Ottawa, Canada.

Abstract

Zircon crystallization ages for a syntectonic granite and an associated dyke along the Tangtse strand of the Karakorum fault are of 18.5 ±0.2 Ma and 18.6±0.2 Ma, respectively. A dyke crosscutting the foliation in the Karakorum shear zone yield an age of 16.0 ± 0.6 Ma. These data show that the Karakorum shear zone was associated with significant granitic magmatism and was active before 16 Ma, since at least ~18.5 Ma. Considering other data along the Karakorum fault, the fault is most likely active since ~22.7 to 25 Ma at a rate of 8 to 13 mm/yr. This study conducted in the frontal part of the Himalayan orogen shows that large continental strike-slip faults can be linked with magmatism, and be stable for more than 20 Ma, even in the hottest part of orogens where strain localisation is supposed to be minimum.

Introduction

The rate and lifespan of intra-continental strike-slip faults is the subject of a long-standing debate. Some have suggested that such faults play a major role in the continental deformation (e.g., Tapponnier et al., 1986; Tapponnier et al., 2001), whereas others consider such faults as transient features accommodating limited deformation (e.g., England and Houseman, 1986). In the India / Eurasia collision zone this debate has mostly focussed on the late Holocene deformation rates along the main strike-slip faults, with some advocating for fast strike-slip rates (e.g., Chevalier et al., 2005; Mériaux et al., 2005) and others for nearly continuous deformation with minor faulting (e.g., Wallace et al., 2004; Wright et al., 2004; Zhang et al., 2004). A complementary approach to the problem is to discuss the life span, total amount of motion, and lithospheric or crustal nature of such faults over longer time scales of several millions years. To this respect, the nature, life span and offset of the Karakorum shear zone (Ksz) (Fig. 1a), have been lively discussed (e.g., Lacassin et al., 2004b). A related discussion stands on the ability or not, of these faults to produce and /or channel melts towards the surface (e.g., Hutton and Reavy, 1992; Leloup et al., 1999; Paterson and Schmidt, 1999).

The Karakorum Fault, is a more than 900km long strike-slip faults bounding Tibet to the SE (KF; Fig. 1a; Fig. 2a). It has been suggested that the KF is active since ~ 23 Ma with synkinematic magmatism occurring at that time in the North Ayilari range (NA in Fig. 2a) (Lacassin et al., 2004a; Valli et al., 2008). On the other hand, Phillips et al. (2004) proposed that 200 km away along strike of the fault near Tangtse (T in Fig. 2a), deformation postdates magmatism, starting after 15.7 Ma and lasting less than 2 Ma. This view, of a recent and short-

lived ductile deformation, that appears to have been widely accepted (Ravikant, 2006; Phillips and Searle, 2007; Rutter et al., 2007; Bhutani et al., 2009; Streule et al., 2009; Wang et al., 2009) has important bearings on the continental collision history and mechanics. Here we present data demonstrating that right-lateral deformation, that is still active today, started more than 18 Ma ago near Tangtse, and suggesting that there are close spatial and temporal relationships between strike-slip shearing and magmatism.

The Karakorum shear zone at Tangtse, relationships between magmatism and deformation.

In Ladakh, the main geological units trend WNW-ESE and are deflected and offset by the NW-SE right-lateral KF (Fig. 2a). The 120 km offset of the Indus River across the fault (Gaudemer et al., 1989) (Fig. 2a) most likely corresponds to the fault motion since 16 to 12 Ma ago (Valli et al., 2007). Correlations of geological units across the KF are not well established and the total offset has been debated, with estimates ranging from no offset (Jain and Singh, 2008) to 1000km (Peltzer and Tapponnier, 1988). Searle et al. (1998) proposed a maximum offset of 120–150 km by correlating the Baltoro and Tangtse granites (Fig. 2a). However, this correlation, if correct, would only provide a minimum offset as the 15.55±0.74 Ma old (Phillips et al., 2004) Tangtse granite is located between the two strands of the KFZ and postdate the KF initiation (This study). The large-scale warping of the Lower Cretaceous Shyok – Shiquanhe suture zone, the Cenozoic Indus – Tsangpo suture zone, and the Mesozoic Ladakh – Gangdese Mesozoic calc-alkaline batholith suggests an offset of 200 (Ratschbacher et al., 1994) to 240 km (Valli et al., 2008) (offset on Fig. 2a).

Near Tangtse (T, Fig. 2a), deformed plutonic, migmatitic and metamorphic rocks including mylonites outcrop in the Pangong range (Fig. 1b). They exhibit a foliation trending N131°, 84° SE on average with a stretching lineation dipping ~15° to the NW (Fig. 1b). These rocks correspond to the ~8 km right-lateral Ksz (e.g., Searle et al., 1998; Rolland and Pêcher, 2001; Phillips and Searle, 2007; Rolland et al., 2009), framed to the SW and NE by the Tangtse and the Muglib mylonitic strands (Fig. 1b). Morphological evidence indicates active right-lateral faulting along the Muglib strand (Brown et al., 2002). Note that the various authors give different names to the geologic formations. We use the names given on Fig. 1.

Mylonitic marbles, calcsilicates and orthogneiss outcrop on the Tangtse strand of the Ksz, around the Tangtse monastery (Fig. 1b). There, Phillips et al. (2004) obtained U/Pb ID-TIMS zircon and Monazite ages of 15.63±0.52 Ma from a mylonitised leucocratic dyke (sample

P11; Table A1; Fig. 1b) and 13.74±0.29 Ma from a cross-cutting dyke (sample P8). They concluded that ductile deformation started after ~ 15.6 Ma and ceased prior to ~ 13.7 Ma. We noted that the cross-cutting dyke is not ~5 km long as depicted by Searle and Phillips (2007), but less than 5 m with two asymmetric tails compatible with right-lateral ductile deformation. The fact that the dyke crosscut the foliation formed by right-lateral shear but is also affected by that deformation implies that it is a synkinematic intrusion. Sample LA60 was taken from another horizontal leucocratic dyke crosscutting the foliation trending N116 (Fig. 3f). Its crystallization age will thus provide a minimum age for the onset of ductile deformation.

The South Tangtse granite (STG) outcropping at the southern margin of the Ksz (Fg. 1b) shows a strong deformation gradient from the SW to the NE (Fig. 3). The STG contains large crystals of K-feldspar, quartz and biotite, and is cut by leucocratic dykes. Both granite and dykes are totally undeformed ~ 400 m south of the Tangtse stand of the Ksz. Towards the Ksz, a faint steep magmatic foliation trending N130 to N105 is defined by the preferred orientation of large K-feldspar crystals and mafic enclaves (Fig. 3c, d). Farther to the NE, both granite and leucocratic dykes show a progressively stronger foliation, which becomes mylonitic trending N125, 70 SW (Fig. 3e), with a lineation dipping ~12° to the NW and right-lateral shear criteria. NE of this outcrop all rocks are strongly deformed and locally contain thin mafic layers with a foliation trending N110 to N130 and lineation close to horizontal (Fig. 1c). The evidence presented in the STG including the progressive deformation increase towards the Ksz and the occurrence of a magmatic foliation parallel to the Ksz and to the mylonitic foliation, is diagnostic of a syntectonic intrusion that will provide a minimum age for deformation.

Emplacement ages of syntectonic granitoids in the Tangtse strand of the Karakorum shear zone.

Zircon grains from samples LA20 (leucocratic dyke) and LA21 (granite) of the undeformed part of the STG, as well as from sample LA60 were dated with the SHRIMP II at the Geological Survey of Canada during two sessions. Analytical procedures and detailed analysis of the data are given in appendix A1, a summary of the results in Table 1 and detailed results in Table A2.

Zircons from sample LA21b show typical magmatic growth zoning in cathodoluminescent images, with some grains showing high-U cores and the evidence of resorption before re-growth (Fig. 4b). One core yield an age of 310±5 Ma (Carboniferous), while 11 rim spots yield a lower intercept age of 18.5±0.2 Ma (MSWD = 2.07, common Pb

anchored upper intercept) (Fig. 4b), which we consider as the best age approximation for these rims, and for the granite final crystallization.

Zircon from an undeformed dyke (LA20) collected at the same location as LA21b yielded very similar results. The zircon grains are euhedral, well zoned, with rare cores that are partially resorbed (Fig. 4a). One core has an age of 25.6±0.3 Ma, while 17 rim analyses define a regression line in a Tera-Wasserburg plot with a lower intercept at 18.61±0.25 Ma (Fig. 4a). The results suggest the presence of a ~26 Ma inheritance and final magma crystallization at ~18.6 Ma, which is synchronous with the surrounding granite.

Zircons extracted from Sample LA60 are strongly metamict with exsolved uraninite (Fig. 4c), and show very high U contents from 2,900 to 12,700 ppm. For zircon with U contents > 2000 ppm ion probe analytical matrix effect may yield inaccurate old ages if uncorrected (Williams and Hergt, 2000). Correction of such effect yields an age of 16.0 ± 0.6 Ma (6 meas., MSWD = 2.6 - 6 grains) (Fig. 4c). This age is, interpreted as the time of crystallisation of the late dyke.

Deformation timing in the Karakorum shear zone and geodynamic consequences.

Lower Miocene granitic rocks of the Ksz both in Tangtse and Ayilari span in age from ~25 to ~13 Ma, and have been interpreted to be syntectonic to right-lateral shearing (Valli et al., 2008; Weinberg and Mark, 2008; Reichardt et al., 2010) (Fig. 1b, Appendix A2, Table A1). Leucogranites of the Pangong range have been interpreted as the product of synkinematic water-fluxed melting of the Late Cretaceous granodiorites and of the Tangtse meta-sedimentary rocks (Reichardt et al., 2010). This interpretation is contested by some authors that consider that all magmatic rocks within the Ksz, unless few isolated dykes, predate deformation (e.g. Phillips et al., 2004; Searle and Phillips, 2004) and that ductile deformation occurred at temperature below solidus (Phillips and Searle, 2007). In that interpretation, right-lateral shear was mostly restrained between 15.7 and 13.7 Ma and the KF is a transient structure. However, our study shows clear evidences that the 18.5 Ma South Tangtse granite is syntectonic, and that strike-slip deformation started prior to 16 Ma in the Tangtse strand. Within the shear zone, part of the evidence for high-temperature deformation has probably been obscured by overprinting of low temperature structures formed during cooling, as temperature dropped to ~400°C at ~13 Ma (Dunlap et al., 1998) while right-lateral shear pursued. Such evidence has been preserved in the South Tangtse granite because it occurs at the margin of the main deformation zone (Fig. 1b).

The age of syntectonic intrusions imply that the KF initiated prior to 22.7±0.1 Ma in the North Ayilari (sample C32, Valli et al., 2007) and 18.5±0.2 near Tangtse (STG; this study) (Fig. 2b). As the fault is still active this ages yield an integrated slip rate of 8.8 to 13 mm/yr along the central section of KF. At the southern extremity of the main KF strand (SA, Fig. 2a), Murphy et al. (2000), suggested that the South Kailash thrust (SKT on Fig. 2a) was offset 66 ± 5.5 km by the KF. The ~19 - 13 Ma age of that thrust, based on a single K-feldspar Ar-Ar thermal history (Yin et al., 1999), was taken to imply that the KF would be younger than 13 Ma at this location (Fig. 2b) with a slip rate ≥ 5.5±0.4 mm/yr. If this piercing point is correct it would imply a very slow propagation of the fault toward the South (Fig. 2b) and an abrupt decrease of the fault motion toward the Gurla Mandhata (GM), or a slow-down from ~14 to ~4 mm/yr at ~13 Ma. Alternatively, assuming all Miocene intrusions along the KF to be syntectonic would imply a slightly older initiation age, a lower integrated slip-rate (8 – 10 mm/yr), and a faster fault propagation (Fig. 2b) (Valli et al., 2008).

The Ksz appears a good pathway for magma produced deeper in the crust to ascend (e.g., Valli et al., 2008; Weinberg and Mark, 2008; Reichardt et al., 2010). Leech (2008) even proposed that the Ksz acted as a barrier collecting all magmas flowing at mid-crustal level from North Tibet towards the south in the framework of the lower crustal channel flow model. This hypothesis would explain why Himalayan granites are fewer and older west of the GM interpreted as the KF SE tip (Fig. 2a). This hypothesis appears sustained by the fact that the STDS, interpreted as the upper bound of the channel, stopped earlier west of the GM than further east. However, this stop occurs at ~17 Ma, thus ~8 Ma after the initiation of magmatism in the Ksz (Fig. 2b) (Leloup et al., 2010) and it is difficult to link the two events. Alternatively, ductile shear heating in the upper mantle could have triggered partial melting in the lower crust. However numerical simulations suggest that for fault rates of ~10 mm/yr, comparable to what we propose for the KF, it could be the case only for unlikely circumstances: very stiff upper mantle and very fertile lower crust (Leloup et al., 1999). Therefore, we suggest that crustal melts collected by the Ksz resulted from high heat flow resulting from crustal thickening (e.g., Huerta et al., 1998), and /or heat advection following slab breakoff (Mahéo et al., 2009). Melting was probably enhanced by fluid circulation (Reichardt et al., 2010).

Large intracontinental strike-slip faults have long been proposed as major conduits collecting fluids and melts originated in the lower crust or the upper mantle (i.e., Hutton and Reavy, 1992; Leloup et al., 1999 and references therein). Within transpressive orogens such large strike-slip faults promote magmas and hot fluid ascent playing a major role in the crust

evolution (e.g., Hollister and Andronicos, 2006; Pirajno, 2010). Whatever the source of fluid, the upward fluid flow will increase the local thermal gradient, soften the rocks and promote strain localisation within the strike-slip shear zone. As a consequence strain localisation could be enhanced in strike-slip faults that thus could be stable through time and absorb large displacements, as long as boundary conditions do not change considerably. Our data confirm that this was the case for the KF during the last ~25 Ma even though it is located in frontal part of the orogen where the high thermal gradient is expected to promote diffuse deformation rather than strain localisation.

Acknowledgements.

Fieldwork was funded by the CNRS / INSU 3F program. L. Ratschbacher and an anonymous referee are thanked for their reviews. Organizers and participants to the 23rd HKT field excursion in Tangtse are thanked for stimulating discussions on the syntectonic, or not, nature of the granitoids within the Tangtse shear zone. B. Heulin of the French embassy in New Delhi is thanked for his help in sending back the samples.

Tables :

Table 1 U/Pb data summary for LA20, 21 and 60.

Figures captions :

Fig. 1 Structural map of the Karakorum shear zone in the Tangtse area

a) India – Eurasia collision main strike-slip faults: SF, Sagaing; RRF, Red River; XF, Xianshuihe; Ku, Kunlun; ATF, Althyntagh; KF, Karakorum. White arrows and black arrows respectively show active and past sense. Black frame corresponds to Fig. 2. **b)** Structural map of the Tangtse area. UTM 44 projection. **c)** Plot of foliations and lineations in the Tangtse shear zone, along the Tangtse gorge and in the south Tangtse granite (STG). Schmidt diagram, lower hemisphere.

Fig. 2 Geology along the KF and corresponding timing constraints

a) Black framed area of Fig. 1a. SA; South Ayilari (Namru); NA, North Ayilari; T, Tangtse; D, Darbuk; S, Satti,; P, Panamik; Za, Zanskar; Gw, Garwal; GM, Gurla Mandata; LP, Leo Pargil; SKT, South Kailash thrust. Geological units drawn from bibliography and Landsat imagery interpretation. MKT: Main Karakorum thrust corresponding to the Shyok suture zone, MMT: Main Mantle Thrust corresponding to the Indus suture zone **b)** Timing constraints plotted along the fault. U/Pb data and corresponding references are reported in Table A1. Red frames indicate syntectonic granitoids. Timing constraints for the STDS from Leloup et al. (2010).

Fig. 3 Detailed geological cross section of the Tangtse strand of the Karakorum shear zone near Tangtse monastery.

a) Geological cross-section of Ksz Tangtse strand based on field observation. **b to f)** photographs of facies and structures along section. **b)** Undeformed South Tangtse granite (sample LA21) with an undeformed leucocratic dyke (sample LA20). **c)** Faint magmatic foliation (fm) defined by the preferred orientation of coarse-grained K-feldspar. A 5 cm wide compass as a scale. **d)** Magmatic foliation (fm) marked by the orientation of mafic enclaves. A hammer as a scale. **e)** Mylonitic orthogneiss and leucocratic dyke affected by right-lateral deformation (foliation trends N130 72S and lineation dips 10W). View from above, hammer peak gives scale. **f)** Horizontal crosscutting leucocratic dyke (sample LA60). Foliation (Fo) is outlined in black and trends ~N115.

Fig. 4. U/Pb zircon Shrimp II data for samples LA20, LA21b and LA60. See data in Tables A2 & A3. **a&b)** LA20 & LA21b Tera-Wasserburg plots and corresponding regressions. Data error ellipses are at 1σ, grey and black for first and second session respectively. c) LA 60 plot for ^{297}Pb corrected ^{206}Pb/^{238}U ages vs ^{238}U/^{96}Zr$_2$O and regression line indicating a single age of 16.0±0.6 Ma. Data point errors are 1σ. Insets are examples of cathodoluminescence images with corresponding ^{206}U/^{238} ages.

References :

Bhutani, R., Pande, K. and Venkatesan, T.R., 2009. 40Ar–39Ar dating of volcanic rocks of the Shyok suture zone in north–west trans-Himalaya: Implications for the postcollision evolution of the Shyok suture zone *Journal of Asian Earth Sciences*, 34, 168-177.

Brown, E.T., Bendick, R., Bourlès, D.L., et al., 2002. Slip rates of the Karakorum fault, Ladakh, India, determined using cosmic ray exposure dating of debris flows and moraines *Journal of Geophysical Research-Solid Earth*, 107.

Chevalier, M.-L., Ryerson, F.J., Tapponnier, P., et al., 2005. Slip-Rate Measurements on the Karakorum Fault May Imply Secular Variations in Fault Motion *Science*.

Dunlap, W.J., Weinberg, R.F. and Searle, M.P., 1998. Karakorum fault zone rocks cool in two phases *Journal of the Geological Society*, 155, 903-912.

England, P. and Houseman, G., 1986. Finite strain calculations of continental deformation, 2. comparison with the India-Asia collision zone *Journal of Geophysical Research*, 91, 3664-3676.

Gaudemer, Y., Tapponnier, P. and Turcotte, D.L., 1989. River offsets across active strike-slip faults *Annales Tectonicae*, 3, 55 – 76.

Hollister, L.S. and Andronicos, C.L., 2006. Formation of new continental crust in Western British Columbia during transpression and transtension *Earth and Planetary Science Letters*, 249, 29-38.

Huerta, A.D., Royden, L.H. and Hodges, K.V., 1998. The thermal structure of collisional orogens as a response to accretion, erosion, and radiogenic heating *Journal of Geophysical Research-Solid Earth*, 103, 15287–15302.

Hutton, D.H.W. and Reavy, R.J., 1992. Strike-slip tectonics and granitepetrogenesis *Tectonics*, 11, 960–967.

Jain, A.K. and Singh, S., 2008. Tectonics of the southern Asian Plate margin along the Karakoram Shear Zone: Constraints from field observations and U–Pb SHRIMP ages *Tectonophysics*, 451, 186–205.

Lacassin, R., Valli, F., Arnaud, N., et al., 2004a. Large-scale geometry, offset and kinematic evolution of the Karakorum fault, Tibet *Earth and Planetary Science Letters*, 219, 255-269.

Lacassin, R., Valli, F., Arnaud, N., et al., 2004b. Reply to Comment on large-scale geometry, offset and kinematic evolution of the Karakorum fault, TibetQ *Earth and Planetary Science Letters*, 229, 159– 163.

Leech, M.L., 2008. Does the Karakoram fault interrupt mid-crustal channel flow in the western Himalaya? *Earth and Planetary Science Letters*, 276, 314–322.

Leloup, P.H., Ricard, Y., Battaglia, J. and Lacassin, R., 1999. Shear heating in continental strike-slip shear zones: numerical modeling and case studies. *Geophysical Journal International*, 136, 19-40.

Mahéo, G., Blichert-Toft, J., Pin, C., et al., 2009. Partial Melting of Mantle and Crustal Sources beneath South Karakorum, Pakistan: Implications for the Miocene Geodynamic Evolution of the India-Asia Convergence Zone *Journal of Petrology*.

Mériaux, A.-S., Tapponnier, P., Ryerson, F.J., et al., 2005. The Aksay segment of the northern Altyn Tagh fault: Tectonic geomorphology, landscape evolution, and Holocene slip rate *Journal of Geophysical Research-Solid Earth*, 110, 32 PP.

Murphy, M.A., Yin, A., Kapp, P., et al., 2000. Southward propagation of the Karakoram fault system, Southwest Tibet; timing and magnitude of slip *Geology*, 28, 451 – 454.

Paterson, S.R. and Schmidt, K.L., 1999. Is there a close spatial relationship between faults and plutons? *Journal of Structural Geology*, 21, 1131-1142.

Peltzer, G. and Tapponnier, P., 1988. Formation and evolution of strike-slip faults, rifts, and basins during the India-Asia collision: An experimental approach *Journal of Geophysical Research-Solid Earth*, 93, 15,085 – 015,117.

Phillips, R.J., Parrish, R.R. and Searle, M.P., 2004. Age constraints on ductile deformation and long-term slip rates along the Karakoram fault zone, Ladakh *Earth and Planetary Science Letters*, 226, 305-319.

Phillips, R.J. and Searle, M.P., 2007. Macrostructural and microstructural architecture of the Karakoram fault: relationship between magmatism and strike-slip faulting *Tectonics*, 26.

Pirajno, F., 2010. Intracontinental strike-slip faults, associated magmatism, mineral systems and mantle dynamics: examples from NW China and Altay-Sayan (Siberia) *Journal of Geodynamics*, 50, 325-346.

Ratschbacher, L., Frisch, W., Liu, G. and Cheng, C.C., 1994. Distributed deformation in Southern and Western Tibet as result of the India-Asia collision *Journal of Geophysical Research-Solid Earth*, 99, 19,917 – 919,945.

Ravikant, V., 2006. Utility of Rb–Sr geochronology in constraining Miocene and Cretaceous events in the eastern Karakoram, Ladakh, India *Journal of Asian Earth Sciences*, 27, 534–543.

Reichardt, H., Weinberg, R.F., Andersson, U.B. and Fanning, M.C., 2010. Hybridization of granitic magmas in the source: The origin of the Karakoram Batholith, Ladakh, NW India *Lithos*, 116, 249-272.

Rolland, Y., Mahéo, G., Pêcher, A. and Villa, I.M., 2009. Syn-kinematic emplacement of the Pangong metamorphic and magmatic complex along the Karakorum Fault (N Ladakh) *Journal of Asian Earth Sciences*, 34, 10–25.

297 Rolland, Y. and Pêcher, A., 2001. The Pangong granulites of the Karakoram Fault (Western
298 Tibet): vertical extrusion within a lithosphere-scale fault? *Comptes rendus de l'académie*
299 *des sciences de Paris*, 332, 363–370.

300 Rutter, E.H., Faulkner, D.R., Brodie, K.H., et al., 2007. Rock deformation processes in the
301 Karakorum fault zone, Eastern Karakoram, Ladakh, NW India *Journal of Structural*
302 *Geology*, 29, 1315-1326.

303 Searle, M.P. and Phillips, R.J., 2004. A comment on Large-scale geometry, offset, and
304 kinematic evolution of the Karakoram fault, Tibet Q by R. Lacassin et al. *Earth and*
305 *Planetary Science Letters*, 219, 255–269.

306 Searle, M.P. and Phillips, R.J., 2007. Relationships between right-lateral shear along the
307 Karakoram fault and metamorphism, magmatism, exhumation and uplift: evidence from
308 the K2–Gasherbrum–Pangong ranges, north Pakistan and Ladakh *Journal of the*
309 *Geological Society*, 164, 439–450.

310 Searle, M.P., Weinberg, R.F. and Dunlap, W.J., 1998. Transpressional tectonics along the
311 Karakoram fault zone, northern Ladakh: constraints on Tibetan extrusion. In:
312 *Continental Transpressional and Transtensional Tectonics* (R.E. Holdsworth, S.R. A.
313 and J.F. Dewey eds).

314 Streule, M.J., Phillips, R. J., Searle, M.P., et al., 2009. Evolution and chronology of the Pangong
315 Metamorphic Complex adjacent to the Karakoram Fault, Ladakh: constraints from
316 thermobarometry, metamorphic modelling and U–Pb geochronology *Journal of the*
317 *Geological Society*, 166, 919–932.

318 Tapponnier, P., Peltzer, G. and Armijo, R., 1986. On the mechanics of the collision between
319 India and Asia. In: *Collision Tectonics* (M.P. Coward and A.C. Ries, eds). Geological
320 Society, London.

321 Tapponnier, P., Zhiqin, X., Roger, F., et al., 2001. Oblique stepwise rise and growth of the Tibet
322 plateau *Science*, 294, 1671-1677.

323 Valli, F., Arnaud, N., Leloup, P.H., et al., 2007. 20 million years of continuous deformation
324 along the Karakorum fault, Western Tibet: a thermochronological analysis *Tectonics*, 26.

325 Valli, F., Leloup, P.H., Paquette, J.-L., et al., 2008. New U-Th/Pb constraints on timing of
326 shearing and long-term slip-rate on the Karakorum fault *Tectonics*, 27.

327 Wallace, K., Yin, G. and Bilham, R., 2004. Inescapable slow slip on the Altyn Tagh fault
328 *Geophysical Research Letters*, 31, 4 PP.

329 Wang, S., Fang, X., Lai, Q., et al., 2009. New radiometric dating constrains the time for
330 initiation of the Karakorum fault zone (KFZ), SW Tibet *Tectonophysics*.

331 Weinberg, R.F. and Mark, G., 2008. Magma migration, folding, and disaggregation of
332 migmatites in the Karakoram Shear Zone, Ladakh, NW India *Geological Society of*
333 *America Bulletin*, 120, 994–1009.

Williams, I.S. and Hergt, J.M., 2000. U-Pb dating of tasmanian dolerites: a cautionary tale of SHRIMP analysis of high-U zircon. In: *New frontiers in Isotope Geoscience* (J.D. Woodhead, J.M. Hergt and W.P. Noble, eds), Lorne.

Wright, T.J., Parsons, B., England, P.C. and Fielding, E.J., 2004. InSAR Observations of Low Slip Rates on the Major Faults of Western Tibet *Science*, 305, 236-239.

Yin, A., Harrison, T.M., Murphy, M.A., et al., 1999. Tertiary deformation history of southeastern and southwestern Tibet during the Indo-Asian collision *Geological Society of America Bulletin*, 111, 1644 – 1664.

Zhang, P.-Z., Shen, Z., Wang, M., et al., 2004. Continuous deformation of the Tibetan Plateau from global positioning system data *Geology*, 32, 809-812.

Site	Sample						Session	Average 206Pb/238U age 207 Pb corrected				Session	207Pb/206Pb vs 238U/206Pb (Tera-Wesserburg) age					interpretation
	Number	Rock type	Characteristics	Localisation (UTM. WGS84) Zone	X	Y		Age (Ma)	MSWD	Number of spots/ grains	Spots (crystal n°, border (b) or core (c))		Lower intercept (Ma)	Upper intercept (Ma)	MSWD	Number of spots/ grains	Common lead anchored	
South Tangts granite	LA20	Leucocratic dike	undeformed	44	238815	3768161	2	**18.6 ± 0.2**	2.18	10/10	*1b, 2b, 5b, 10b, 11b, 14b, 18b, 19b, 20b, 21b*	1 & 2	18.6 ± 0.3	5139 ± 150	1.8	17/14	*no*	emplacement age
							1	**25.6 ± 0.3**	-	1/1	*17c*							inherited age
South Tangtse granite	LA21b	Granite	undeformed	44	238815	3768161	2	**18.5 ± 0.2**	2.07	11/11	*2b, 4b, 5b, 6b, 8b, 9b, 11b, 22b, 25b, 26b, 28b*	1 & 2	18.6 ± 0.2	5158 ± 170	1.8	19/19	*no*	emplacement age
							1	**310 ± 5**	-	1/1	*20c*							inherited age
								Age vs U(ppm) age										
								Intercept at 2000ppm (Ma)	MSWD	Number of spots/ grains	Spots (crystal n°/ border (b) or core (c))							
Tangtse strand	LA60	Leucocratic dike	cross cutting	44	239212	3768440	1	**16.0 ± 0.6**	2.6	6/6	*2b, 3b, 4b, 6b, 14b, 17b*							emplacement age

Table 1

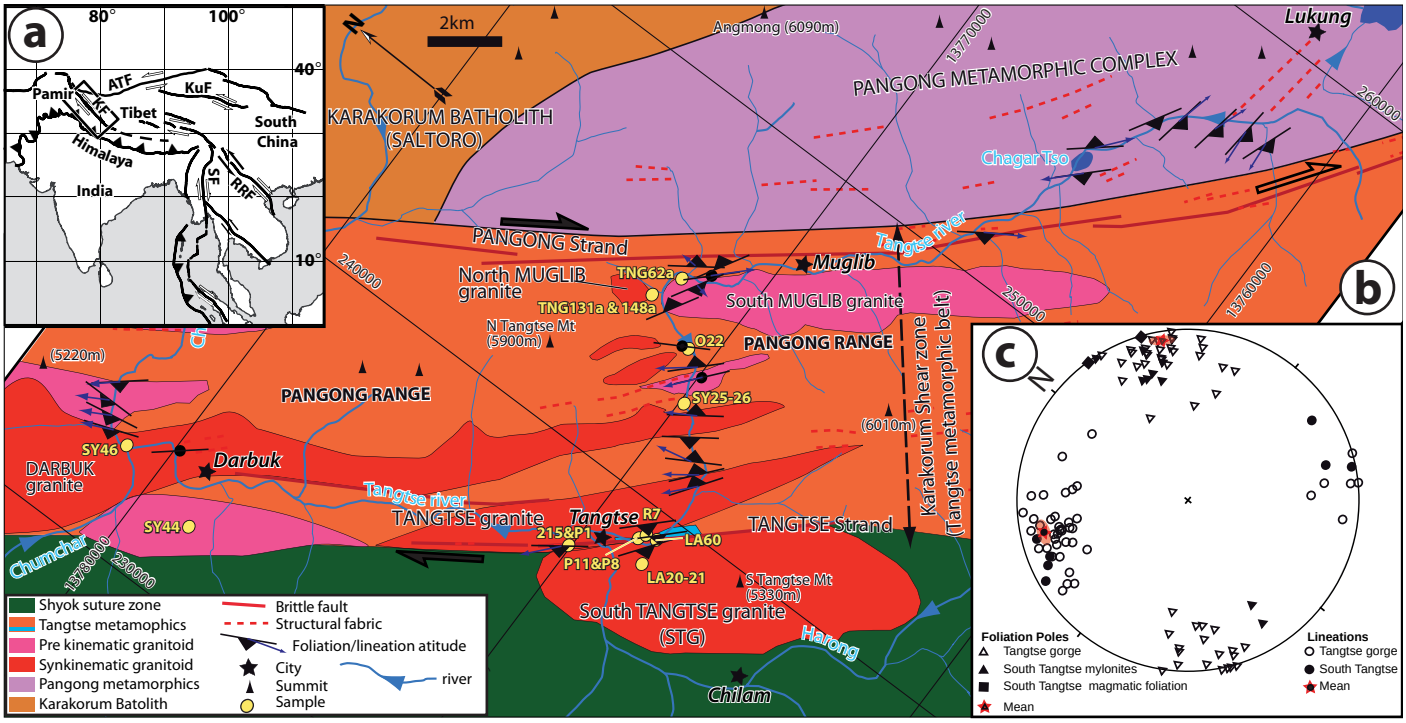
a
80°
100°
40°
10°
Pamir
ATF
KuF
KF
Tibet
South China
Himalaya
India
SF
RRF
2km
KARAKORUM BATHOLITH (SALTORO)
Angmong (6090m)
PANGONG METAMORPHIC COMPLEX
Lukung
Chagar Tso
PANGONG Strand
Tangtse river
Muglib
North MUGLIB granite
TNG62a
TNG131a & 148a
South MUGLIB granite
N Tangtse Mt (5900m)
O22
PANGONG RANGE
b
(5220m)
PANGONG RANGE
SY25-26
(6010m)
Karakorum Shear zone (Tangtse metamorphic belt)
SY46
Darbuk
DARBUK granite
Tangtse river
TANGTSE granite
Tangtse
R7
215&P1
LA60
TANGTSE Strand
SY44
Chumchar
P11&P8
LA20-21
S Tangtse Mt (5330m)
South TANGTSE granite (STG)
Harong
Chilam
240000
250000
260000
1377000
1376000
c
Foliation Poles
Tangtse gorge
South Tangtse mylonites
South Tangtse magmatic foliation
Mean
Lineations
Tangtse gorge
South Tangtse
Mean
Shyok suture zone
Tangtse metamophics
Pre kinematic granitoid
Synkinematic granitoid
Pangong metamorphics
Karakorum Batolith
Brittle fault
Structural fabric
Foliation/lineation atitude
City
Summit
Sample
river

Figure 1

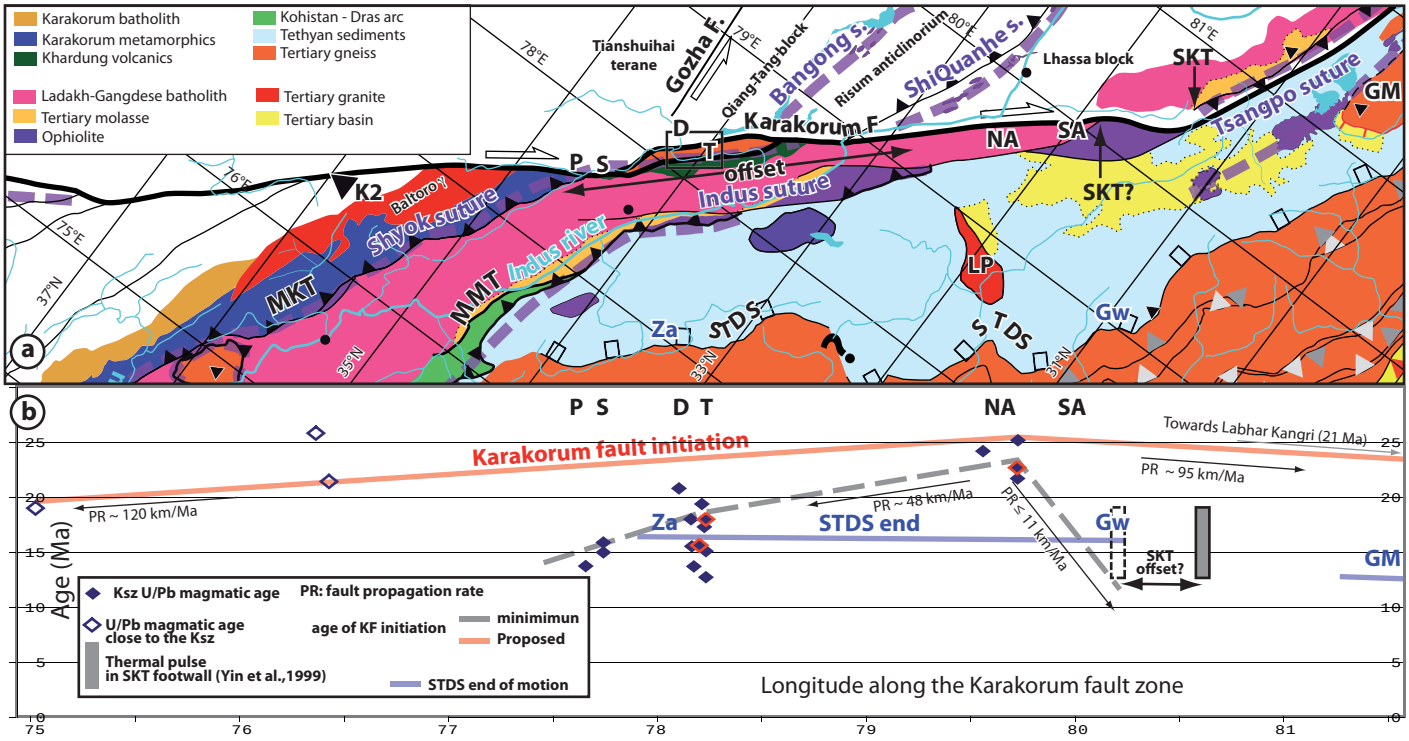
Karakorum batholith
Karakorum metamorphics
Khardung volcanics
Ladakh-Gangdese batholith
Tertiary molasse
Ophiolite
Kohistan - Dras arc
Tethyan sediments
Tertiary gneiss
Tertiary granite
Tertiary basin
Tianshuihai terane
Gozha F.
Qiang-Tang block
Bangong s.
Risum anticlinorium
ShiQuanhe s.
Lhassa block
SKT
GM
Tsangpo suture
Karakorum F.
D
T
P
S
NA
SA
offset
Indus suture
SKT?
K2
Baltoro γ
Shyok suture
MKT
MMT
Indus river
LP
Za
STDS
Gw
a
78°E
79°E
80°E
81°E
76°E
75°E
37°N
35°N
33°N
31°N

b
P S
D T
NA SA
Towards Labhar Kangri (21 Ma)
Karakorum fault initiation
PR ~ 120 km/Ma
PR ~ 48 km/Ma
PR ~ 95 km/Ma
PR ≤ 11 km/Ma
Za
STDS end
Gw
SKT offset?
GM
Age (Ma)
Ksz U/Pb magmatic age
U/Pb magmatic age close to the Ksz
Thermal pulse in SKT footwall (Yin et al.,1999)
PR: fault propagation rate
age of KF initiation
minimimun
Proposed
STDS end of motion
Longitude along the Karakorum fault zone
0
5
10
15
20
25
75
76
77
78
79
80
81

Fig. 2

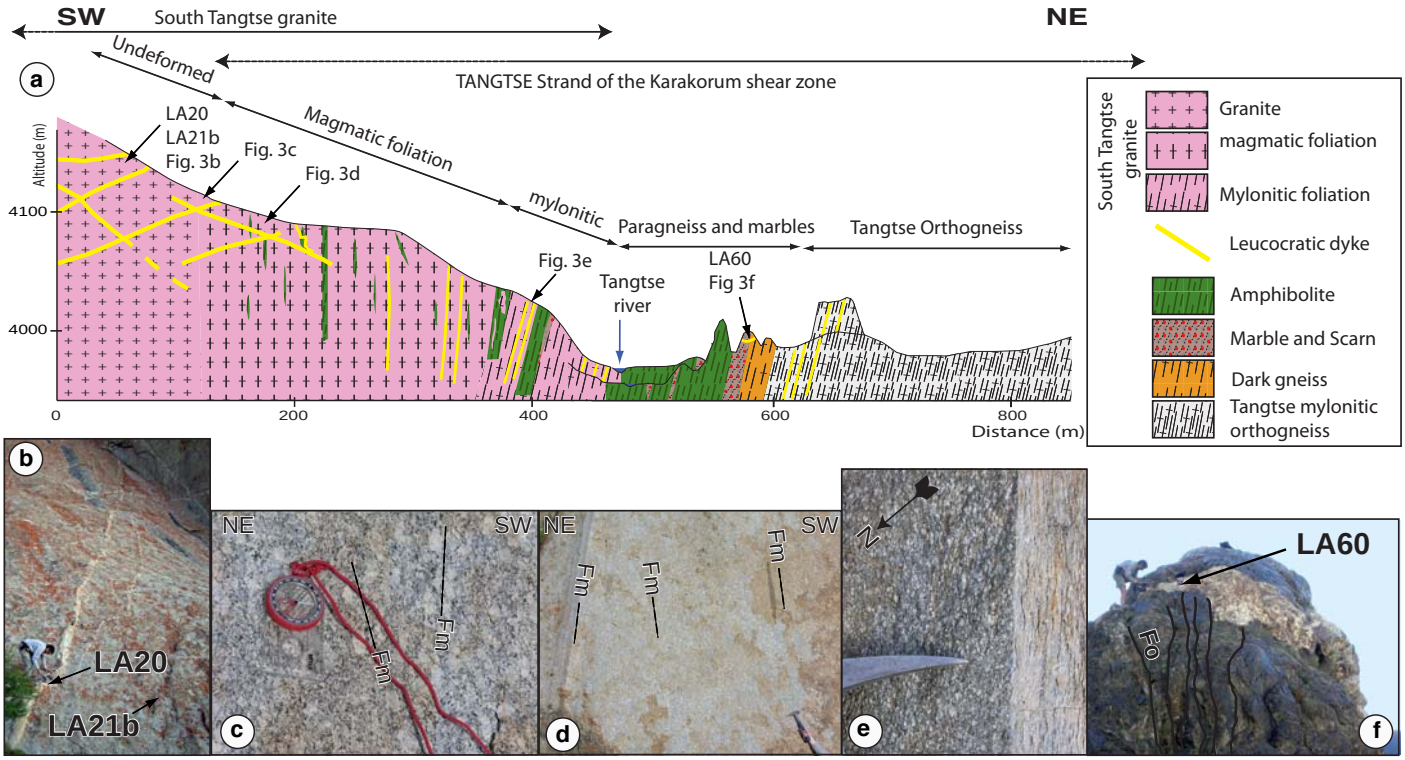
SW
South Tangtse granite
NE
a
Undeformed
TANGTSE Strand of the Karakorum shear zone
Magmatic foliation
mylonitic
LA20
LA21b
Fig. 3b
Fig. 3c
Fig. 3d
Fig. 3e
Tangtse river
LA60
Fig 3f
Paragneiss and marbles
Tangtse Orthogneiss
Altitude (m)
4100
4000
0
200
400
600
800
Distance (m)
South Tangtse granite
Granite
magmatic foliation
Mylonitic foliation
Leucocratic dyke
Amphibolite
Marble and Scarn
Dark gneiss
Tangtse mylonitic orthogneiss
b
LA20
LA21b
NE
SW
Fm
c
d
e
N
LA60
Fo
f

Fig. 3

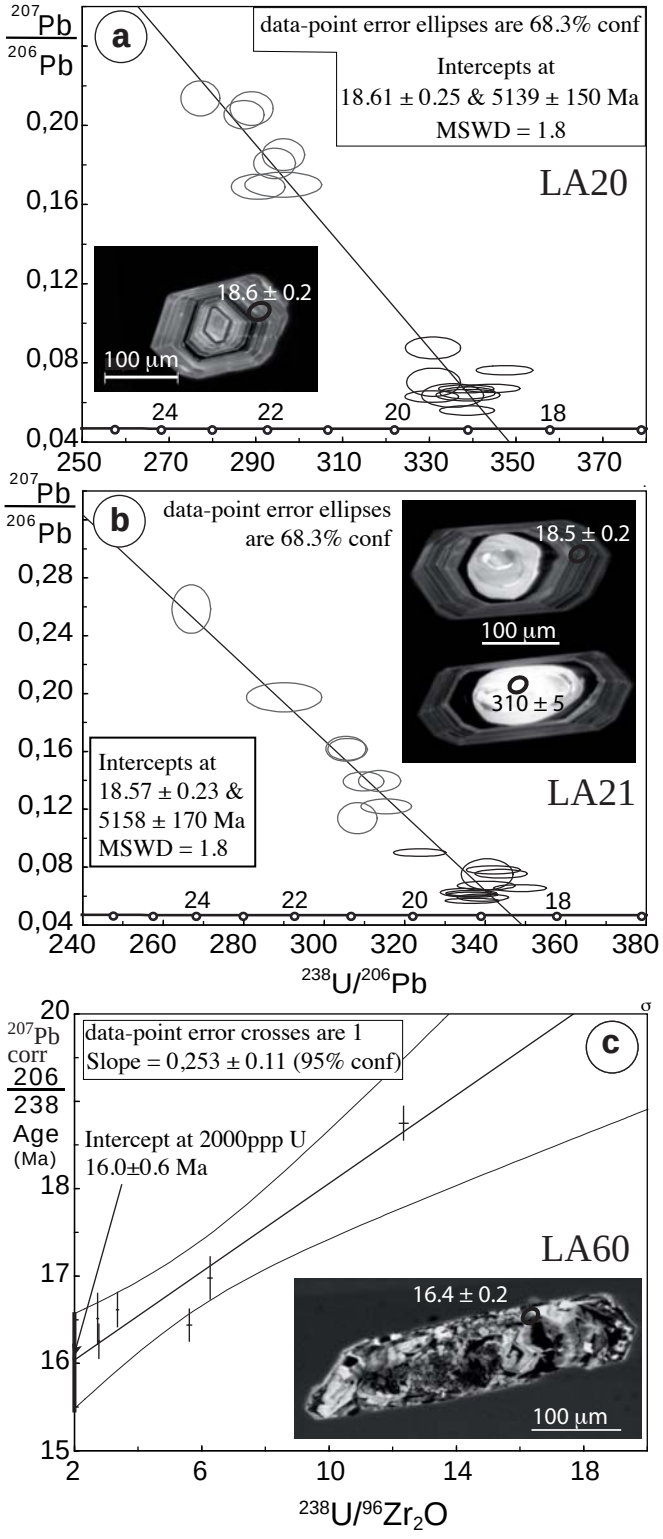
a
data-point error ellipses are 68.3% conf
Intercepts at
18.61 ± 0.25 & 5139 ± 150 Ma
MSWD = 1.8
LA20
18.6 ± 0.2
100 µm
b
data-point error ellipses
are 68.3% conf
18.5 ± 0.2
100 µm
310 ± 5
Intercepts at
18.57 ± 0.23 &
5158 ± 170 Ma
MSWD = 1.8
LA21
c
data-point error crosses are 1
Slope = 0,253 ± 0.11 (95% conf)
Intercept at 2000ppp U
16.0±0.6 Ma
LA60
16.4 ± 0.2
100 µm
207Pb/206Pb
238U/206Pb
207Pb corr 206/238 Age (Ma)
238U/96Zr2O

Fig. 4